Maspin Retards Cell Detachment via a Novel Interaction with the Urokinase-Type Plasminogen Activator/Urokinase-Type Plasminogen Activator Receptor System

Shuping Yin,[1] Jaron Lockett,[1] Yonghong Meng,[1] Hector Biliran, Jr.,[1] Grant E. Blouse,[3,4] Xiaohua Li,[1] Neelima Reddy,[1] Zimin Zhao,[1] Xinli Lin,[5] John Anagli,[3,4] Michael L. Cher,[1,2,3] and Shijie Sheng[1,3]

Departments of [1]Pathology and [2]Urology and [3]The Barbara Ann Karmanos Cancer Institute, Wayne State University School of Medicine; [4]Department of Pathology, Henry Ford Health System, Detroit, Michigan; and [5]ProteomTech, Inc., Emeryville, California

Abstract

It is well documented that tumor suppressive maspin inhibits tumor cell invasion and extracellular matrix remodeling. Maspin is a cytosolic, cell surface–associated, and secreted protein in the serine protease inhibitor superfamily. Although several molecules have been identified as candidate intracellular maspin targets, the extracellular maspin target(s) remains elusive. Although maspin does not directly inhibit urokinase-type plasminogen activator (uPA) activity, we have shown evidence that maspin may block the pericellular proteolysis mediated by cell surface–associated uPA. In the current study, maspin significantly inhibited the Ca^{2+} reduction–induced detachment of DU145 cells. This maspin effect was associated with increased and sustained levels of mature focal adhesion contacts (FAC). We noted that maspin (*a*) colocalized with uPA and uPA receptor (uPAR), (*b*) enhanced the interaction between uPAR and low-density lipoprotein receptor related protein, and (*c*) induced rapid internalization of uPA and uPAR. The maspin effects on surface-associated uPA and uPAR required the interaction between uPA and uPAR. Further biochemical and biophysical analyses revealed that maspin specifically bound to pro-uPA with a deduced K_d of 270 nmol/L and inhibited the plasmin-mediated pro-uPA cleavage. Interestingly, substitution of maspin p_1' site Arg^{340} in the reactive site loop (RSL) with alanine not only abolished the binding to pro-uPA but also diminished the maspin effects on pro-uPA cleavage and cell detachment. These data show an important role of maspin RSL in regulating the uPA/uPAR–dependent cell detachment. Together, our data led to a new hypothesis that maspin may stabilize mature FACs by quenching localized uPA/uPAR complex before uPA activation. (Cancer Res 2006; 66(8): 4173-81)

Introduction

Maspin is a novel serine protease inhibitor (serpin; refs. 1–3). Its expression is epithelial specific and predicts a better prognosis for prostate, colon, thyroid, lung, and oral squamous cancers (reviewed in ref. 4). Maspin reexpression or treatment restores differentiated epithelial phenotypes (5, 6). Consistently, accumulated evidence shows that maspin inhibits tumor cell motility and invasion *in vitro* (3, 5, 7–11) and inhibits tumor growth and metastasis *in vivo* (3, 6). Maspin is also shown to inhibit tumor-induced angiogenesis (12–14).

Maspin is a secreted, cell surface–associated, and intracellular molecule. The biological functions of maspin seem to depend on its subcellular localization. Intracellular maspin is shown to sensitize tumor cells to drug-induced apoptosis (15, 16) and regulate the signaling pathways involved in actin filament dynamics (8). Not surprisingly, several molecules identified as candidate intracellular maspin partners support a role of maspin as a stress regulator (17, 18). On the other hand, the maspin effect on tumor cell motility and invasion seems to be localized to the cell surface and depend on cell interaction with the extracellular matrix (ECM; ref. 10).

A current consensus suggests that cell motility and invasion require both the dynamic formation of new adhesion and the detachment from matured (or established) cell-matrix interaction (19). In fact, mature focal adhesion contacts (FAC) have been shown to retard cell detachment and limit cell migration (20). *In vitro* studies have shown that maspin enhances cell adhesion to ECM protein fibronectin with increased FACs (5, 8). Because increased cell adhesion dynamics in the absence of detachment control may lead to a net increase of cell migration and invasion, the maspin effect on cell adhesion to fibronectin *alone* can not adequately explain the inhibitory effect of maspin on cell motility and invasion.

Previously, we showed that maspin inhibits the activity of cell surface–associated urokinase-type plasminogen activator (uPA). The inhibitory effect of maspin on cell surface–associated uPA activity correlates with its effect on cell motility and invasion (21). uPA together with uPA receptor (uPAR) are known to play multifaceted roles to facilitate pericellular proteolysis and oncogenic signal transduction (22, 23). Recently, we and others also showed that maspin is robustly internalized (7, 18). These data raised the question whether maspin internalization regulates the cell surface biochemical presentation of the uPA/uPAR complex and/or the cell-matrix interaction.

The current report describes the first evidence that maspin strengthens mature FACs and retards cell detachment. Binding of maspin to the cell surface depends on its specific interaction with the uPA/uPAR complex and subsequently triggers a rapid low-density lipoprotein receptor–related protein (LRP)–dependent internalization. We also provide the first evidence that maspin has a novel preference for pro-uPA and inhibits plasmin-mediated pro-uPA cleavage. Our data suggest that maspin may regulate the dynamics of FACs by quenching localized uPA/uPAR complex before the initiation of an uPA-dependent proteolytic cascade.

Note: S. Yin and J. Lockett contributed equally to this work.

Requests for reprints: Shijie Sheng, Department of Pathology, Wayne State University School of Medicine, 540 East Canfield Avenue, Detroit, MI 48201. Phone: 313-993-8197; Fax: 313-993-4112; E-mail: ssheng@med.wayne.edu.

doi:10.1158/0008-5472.CAN-05-3514

Materials and Methods

Chemicals and reagents. Maspin (11), a polyclonal antibody against maspin reactive site loop (RSL; Abs4A), and a polyclonal antibody against maspin s3A peptide (Abs3A) were produced as previously described (3). Pro-uPA was from ProteomTech, Inc. (Emeryville, CA). Two-chain active uPA and recombinant plasminogen activator inhibitory type I (rPAI-1) were from Abbott Laboratories (Chicago, IL). Monoclonal antibody to the β-chain of human LRP was from Maine Biotechnology (Portland, ME). Monoclonal antibodies to maspin, focal adhesion kinase (FAK), and phospho-FAK (Y^{397}) were from BD Biosciences (San Diego, CA). Fluorescein-5-EX succinimidyl ester (F-6130), fluorescently conjugated secondary antibodies, and the Antifade kit were from Molecular Probes (Eugene, OR). Peroxidase-conjugated anti-mouse IgG and anti-rabbit IgG and the enhanced chemiluminescence detection kit were from Amersham (Piscataway, NJ). Reagents from American Diagnostica (Greenwich, CT) include plasmin, polyclonal anti-human uPA antibody, polyclonal anti-uPAR antibody (399R), and monoclonal antibody against the amino terminal fragment of uPA (anti-uPA ATF). Reagents for protein concentration analysis and SDS-PAGE were from Bio-Rad (Hercules, CA). Cycloheximide, phosphatidylinositol-specific phospholipase C (PI-PLC), sulforhodamine B, and other chemicals were from Sigma (St. Louis, MO).

Cell cultures. Human prostate cancer cell line DU145-derived maspin-transfected clones (M3, M7, and M10) and the mock-transfected clone (Neo) were generated in our earlier study (7). Both DU145 cells and the DU145-derived transfected clones were maintained in RPMI 1640 supplemented with 5% fetal bovine serum. An additional 300 μg/mL of G418 was added to the culture media for the transfected clones. Normal human prostate epithelial cells CRL2220 (American Type Culture Collection, Manassas, VA) were cultured in serum-free keratinocyte growth medium (KGM-SF). Culture media and components were from Invitrogen (Gaithersburg, MD). All cell cultures were kept in a humidified incubator at 37°C with 6.5% CO_2. Cell growth was monitored by cell counting using a Coulter particle counter Model Z1 (Beckman, Fullerton, CA). In colonogenicity assay, transfected cells were seeded in six-well plates at a low density of 100 per well and incubated for 5 days.

Quantification of secreted endogenous maspin. KGM-SF conditioned by CRL2220 cells were collected at various time points. The concentrated conditioned media along with purified recombinant maspin (rMaspin) standards were subjected to Western blotting for maspin. The amounts of maspin secreted by CRL2220 cells were estimated using a standard curve constructed based on densitometric measurements of rMaspin standards on the same Western blot membrane.

Expression and purification of Mas^{R340A}. Using the Exsite PCR-Based Site-Directed Mutagenesis kit (Stratagene, La Jolla, CA), we substituted wild-type maspin Arg^{340} in the pVL1393/mas template (11) with an alanine. The PCR primers for mutagenesis were 5′-CCATAGAGGTGCCAGGAG-CAGCGATCCTGCAGCACAAGG-3′ and 5′-CCTTGTGCTGCAGGATCGC-TGCTCCTGGCACCTCTATGG-3′. The resulting sequence-verified maspin mutant, Mas^{R340A}, was expressed in baculovirus-infected insect cells and purified as previously described (11).

Adenoviral expression of maspin. The full-length maspin cDNA was flanked by *Bgl*II restriction enzyme and inserted into the pAdeno-VatorCMV5 transfer plasmid (AdenoVator kit, Q-Bio Gene, Carlsbad, CA). The resulting transfer vector, verified for orientation and sequence fidelity, was used along with pAdenoVatorΔE1/E3 vector for *Escherichia coli* cotransfection to generate the recombinant adenoviral DNA, designated as Ad-CMV-mas. Parallel cotransfection with the empty transfer vector pAdenoVatorCMV5 and the pAdenoVatorΔE1/E3 vector produced the control adenoviral DNA, Ad-CMV. The adenoviral DNA were linearized by *Pac*I restriction digestion and used to transfect QBI-293A cells to generate viral clones. After the plaque assay for gene expression, large scales of selected recombinant virus clones were prepared and titrated. One plaque-forming unit was used for routine cell infection.

Cell detachment assay. Cells were seeded in triplicate onto 96-well plates (1.0×10^4 per well), incubated for 24 hours, and washed with PBS. Then the cells were incubated in a Ca^{2+}-reduced isotonic detachment buffer [PBS, 7.5% (v/v) of RPMI 1640, and 10 μg/mL of cycloheximide] for 4 hours in the presence of bovine serum albumin (BSA), rMaspin, or Mas^{R340A}. The adherent cells were washed and photographed using a SPOT digital camera (Diagnostic Instruments, Sterling Heights, MI) under a Leica DM IRB microscope. Then, the cells were stained with sulforhodamine B and quantified by spectrophotometric absorbance at 550 nm (24).

Protein binding to the cell surface. DU145 cells seeded into six-well plates (5.0×10^5 per well) were cultured for overnight and treated with cycloheximide (10 μg/mL) for 1 hour at 37°C. The cells were then treated in the continuous presence of cycloheximide by the following schemes: (*a*) To test the binding of maspin to the cell surface, cells were treated with 20 μg/mL of BSA or 20 μg/mL of rMaspin at 4°C for 1 hour. (*b*) For testing the role of glycosylphosphotidylinositol anchorage, cells were sequentially treated with 5 units/mL of PLC at 37°C for 30 minutes and incubated with 20 μg/mL of rMaspin at 4°C for 1 hour. (*c*) To test the role of cell surface–associated uPA and uPAR, maspin-expressing transfected cells that had been acid stripped (25) were incubated with anti-uPA ATF, anti-uPAR (399R), or preimmune IgG for 16 hours at 37°C. Complementarily, acid-stripped Neo cells were incubated with anti-uPA ATF, anti-uPAR, or preimmune IgG for 16 hours at 37°C and incubated with 20 μg/mL of rMaspin at 4°C for 1 hour. Cell preparations resulting from above treatments will be subjected to Western blot analyses.

Protein internalization. Overnight cell cultures in six-well plates were incubated at 4°C for 2 hours with or without 20 μg/mL of rMaspin. The cells were washed and incubated in KGM-SF containing 10 μg/mL of cycloheximide at 37°C for up to 90 minutes. Conditioned media were concentrated by Centricon-10 filter units (Amicon, Bedford, MA). Half of the cells were lysed in a hypotonic protease inhibitor-rich buffer (26). Another half of the cells were surface biotinylated with sulfo-NHS-biotin (EZ-Link Sulfo-NHS Biotinylation kit, Pierce, Rockford, IL). Cell lysates derived from surface biotinylation were subjected to strepavidin pulldown to separate cell surface-associated proteins (biotinylated) and cytosolic proteins (nonbiotinylated). Finally, all protein fractions were subjected to Western blot analyses.

To track internalized proteins, we did reverse cell surface protein biotinylation. DU145 cells (1.75×10^6 per 100-mm dish) were incubated overnight and washed with ice-cold PBS. The cells were incubated with sulfo-NHS-Biotin for 30 minutes at 4°C and treated with 10 μg/mL of anti-uPAR (399R) or preimmune IgG for 2 hours at 4°C. Next, rMaspin (20 μg/mL) was added to cells and incubated for an additional 2 hours at 4°C. Cells were acid stripped (25) and placed at 37°C. At the indicated time points, cells were resuspended in lysis buffer supplemented with 300 mmol/L sucrose and homogenized on ice with a DOUNCE homogenizer (10 strokes). The cell lysates were subjected to strepavidin affinity pulldown according to the manufacturer's protocol. The resulting pulldown (internalized biotinylated molecules) and run-through (nonbiotinylated) fractions were subjected Western blot analyses.

Immunoprecipitation/Western blot. One milligram of total or fractionated cell extracts was incubated at 4°C for 16 hours with polyclonal antibody to uPA, polyclonal antibody to uPAR, or preimmune IgG at a final concentration of 2.5 μg/mL. Immune complexes were precipitated by protein G/protein A agarose beads (20 μL beads: 1 mL of cell lysate) for 2 hours at 4°C, centrifuged at 2,500 rpm for 5 minutes, washed with cold lysis buffer, and heat denatured in reducing SDS-PAGE sample buffer. The denatured protein samples were analyzed by Western blot.

Confocal immunofluorescence microscopy. To examine the endogenous protein expression, cells in eight-well chamber slides (1.0×10^5 per well) were fixed with 3.8% paraformaldehyde for 10 minutes. Cells were permeabilized with 0.1% saponin in PBS for 10 minutes when indicated. In the case for detecting the total level of endogenous uPA, cells were permeabilized with 0.2% Triton X-100 instead. The cells were then blocked with 2% BSA in PBS for 1 hour at room temperature, washed, and incubated for 1 hour with anti-uPA β-chain (10 μg/mL), anti-uPAR (10 μg/mL), Abs3A (10 μg/mL), or anti-phospho(Tyr^{397})-FAK (10 μg/mL). To investigate the cell surface binding of maspin, DU145 cells were pretreated at room temperature for 2 hours with 20 μg/mL of preimmune IgG, or anti-uPA (10 μg/mL) plus anti-uPAR (10 μg/mL). The cells were then treated with

rMaspin (20 μg/mL, 2 hours, 4°C) before fixation. The bound primary antibodies were blotted with Oregon Green goat anti-rabbit IgG (1:200 dilution) or Texas Red goat anti-mouse IgG (1:100 dilution) for 1 hour. The cells were then washed and mounted with the Prolong Antifade solution. Confocal microscopic examination was done using Zeiss LSM310 Model (The Confocal Imaging Core of KCI, WSU).

ELISA. Ninety-six–well plates were coated with 2.5 μg/well of pro-uPA, plasmin, or BSA (negative control) for 2 hours at room temperature, washed with PBS-T (PBS containing 0.05% Tween 20), and blocked with 100 μL/well of 0.25% BSA for 2 hours at room temperature. The plates were then incubated at 4°C for overnight with rMaspin, Mas^{R340A}, or BSA, each at 2.5 μg/50 μL/well. After three washes, the plate was incubated with maspin monoclonal antibody (1:2,000 dilution) for 2 hours at room temperature. The bound antibody was probed with 1:6,000 diluted horseradish peroxidase–conjugated anti-mouse IgG and quantified based on the reaction with *o*-phenylenediamine substrate that produced spectrophotometric absorbance at 450 nm.

Equilibrium binding of $maspin^{-FL}$ to pro-uPA. rMaspin was randomly labeled on solvent accessible primary amines with fluorescein 5-EX succinimidyl ester. Briefly, a 0.5-mL reaction mixture containing 3.2 μmol/L rMaspin and 32 μmol/L fluorescein 5-EX succinimidyl ester in 0.2 mol/L $NaHCO_3$ (pH 8.3) was incubated for 60 minutes at room temperature and then quenched with 50 μL of 0.75 mol/L hydroxylamine (pH 8.5) for an additional 60 minutes. The excess unreacted probe was removed by dialysis against PBS at 4°C. Each rMaspin was labeled with ~3.5 fluorescein units based on the A_{496} and an $E_{coefficient}$ of 67,500. In equilibrium binding assays, 10 nmol/L of fluorescein labeled maspin ($maspin^{-FL}$) was incubated with pro-uPA at various concentrations for 10 minutes at 25°C. Displacement of noncovalently bound $maspin^{-FL}$ was accomplished by the addition of unlabeled rMaspin to an equilibrated reaction of 10 nmol/L $maspin^{-FL}$ and 0.5 μmol/L pro-uPA. Fluorescence emission spectra were recorded between 500 and 650 nm using an excitation wavelength of 490 nm on a Varian Cary Eclipse fluorescence spectrophotometer equipped with a Peltier-controlled thermostatted cell holder. Data points for equilibrium binding isotherms were determined from the integrated fluorescence peaks as described (27). Binding isotherms were fit to the quadratic equation (27) for equilibrium binding constants.

Cleavage of pro-uPA by plasmin. Pro-uPA and rMaspin (or Mas^{R340A}) were mixed at 1:1 molar ratio in PBS. The resulting mixtures were incubated for 15 minutes at 37°C. Then plasmin was added to the indicated reactions at 1:10 ratio to pro-uPA. In control reactions, PBS was added in the place of plasmin. The final volume of the reaction mixture was 45 μL. These reaction mixtures were incubated for 20 minutes at 37°C, heat denatured in SDS-PAGE sample buffer, and subjected to Western blot analyses.

Miscellaneous. For the equilibrium binding assay, protein concentration was determined by the A_{280} absorbance calibrated with purified rPAI-1 (28). For other experiments, protein concentration was determined by the Bradford method (29). SDS-PAGE and Western blot were done as previously described (11). Densitometry analyses of scanned Western blot images (scanner, UMAX Astra1220U) were done using the NIH Image 1.62 program.

Results

Maspin effect on cell focal adhesion complex and cell detachment. To investigate the molecular mechanisms underlying the inhibitory effects of maspin on tumor cell motility and invasion, we further examined the biological characteristics of DU145-derived transfected cells (7). Compared with the parental and mock-transfected control cell lines, maspin-transfected cells grew at a similar rate (Fig. 1*A, a*). When seeded sparsely, maspin-transfected cell lines and the mock control cell line formed the same numbers of anchorage-dependent colonies (data not shown). However, in contrast to the mock-transfected control colonies that showed significant scattering, colonies of three maspin-transfected clonal cell lines remained tightly clustered (Fig. 1*A, b*). Thus, the inhibitory effect of maspin on cell scattering and motility is not likely associated with changes of growth kinetics.

Earlier investigations suggest that maspin enhances cell adhesion to ECM protein fibronectin *in vitro* (5, 30). However, because the ability of cells to make new attachments may increase

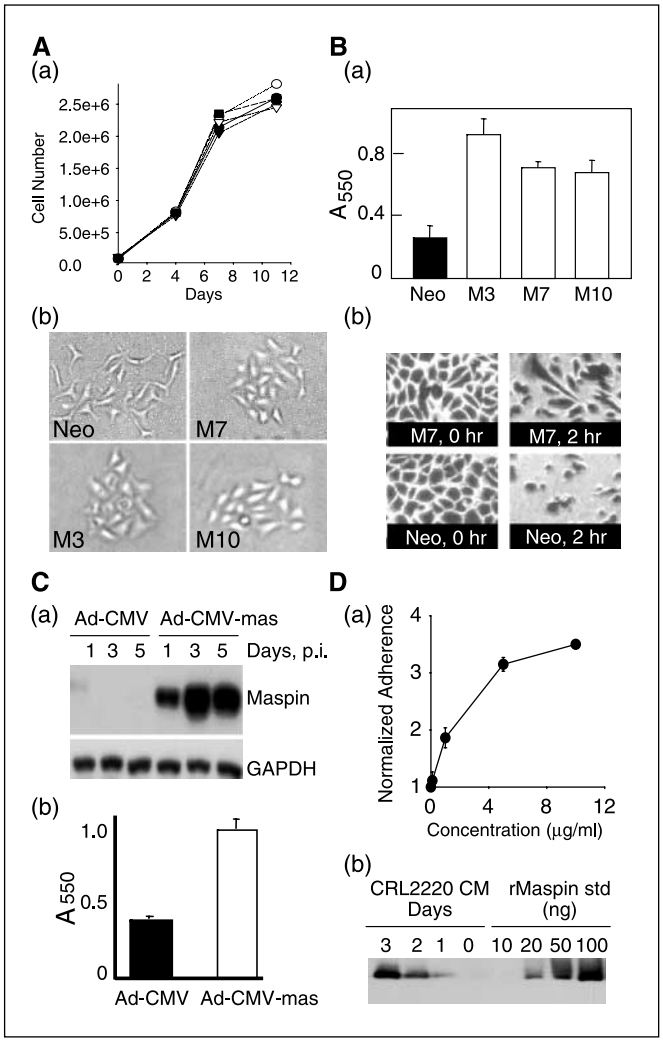

Figure 1. Maspin inhibits cell migration without affecting cell growth. *A,* maspin inhibits cell scattering but not cell growth. *a,* growth curves of parental DU145 cells (○), mock-transfected Neo cells (▽), and three maspin-transfected cell lines M3 (●), M7 (▼), and M10 (■); *b*, representative phase-contrast microscopic images of Neo, M3, M7, and M10 clonal cells in anchorage-dependent colonogenic assay. Magnification, ×200. *B,* maspin reexpression inhibits DU145 cell detachment. *a,* post-detachment measurement of adherent cells by sulforhodamine B assay (A_{550}). *b*, representative microscopic images of sulforhodamine B–stained cells at 0 or 2 hours into the detachment treatment. Magnification, ×200. *C,* adenoviral expression of maspin inhibits cell detachment. *a,* Western blot of maspin in the lysates of cells that had been infected with Ad-CMV or Ad-CMV-mas for the indicated post-infection (*p.i.*) time periods. A total of 30 μg of cell lysate proteins was loaded into each lane. Western blot of glyceraldehyde-3-phosphate dehydrogenase (*GAPDH*) on the same membrane was done to normalize the protein loading. *b,* sulforhodamine B assay (A_{550}) of post-detachment adherent DU145 cells that had been infected for 3 days with Ad-CMV or Ad-CMV-mas. *D, a,* dose-dependent effect of rMaspin on DU145 cell detachment. Post-detachment adherence was quantified by sulforhodamine B assay and normalized by the BSA background at the corresponding concentration. *b,* Western blot/densitometric quantification of maspin secretion by CRL2220. Concentrated culture media (*CM*) conditioned by 1×10^6 cells for the indicated periods of time along with purified rMaspin standard were subjected to denaturing SDS-PAGE and Western blot of maspin. *Points/columns,* average of three repeats; *bars,* SE. The error bars are omitted in (*A, a*) for clarity.

cell motility (31), the maspin effect on cell adhesion to fibronectin does not seem adequate to explain its inhibitory effect on cell motility. Considering that cell movement also involves detachment from the established ECM contacts, we tested the effect of maspin on cell detachment. Divalent cations, especially Ca^{2+}, act as cofactors for integrin-mediated cell-matrix interactions. As shown in Fig. 1*B*, when Ca^{2+} concentration was reduced by ~10-fold, maspin-transfected DU145 cells detached from their native ECM at a significantly slower rate than the mock-transfected cells.

To test whether the retarded detachment of maspin-transfected cells was a result of the selection of surviving stably transfected cell lines or cellular adaptation to long-term maspin expression, we constructed an adenoviral system to deliver maspin expression via acute infection. Adenoviral expression of maspin was not toxic and did not change the cell proliferation rate in the time periods of our experiments (data not shown). On the third day after infection, the level of maspin expression in Ad-CMV-maspin–infected cells reached the plateau (Fig. 1*C, a*). At this time point, cells were treated by the detachment condition. As shown in Fig. 1*C* (*b*), maspin expression was associated with a significant inhibition of cell detachment.

Purified maspin, rMaspin, has been shown to inhibit tumor cell invasion and motility *in vitro* (21). We treated DU145 cells with rMaspin under the detachment condition. As shown in Fig. 1*D* (*a*), rMaspin protected DU145 cells against Ca^{2+} reduction–induced detachment in a dose-dependent manner. rMaspin used at concentrations lower than 1 μg/mL was effective. To determine whether these effective rMaspin concentrations were physiologically relevant, we quantified maspin secreted by normal prostate epithelial cells by Western blot. As shown in Fig. 2*D* (*b*), secreted endogenous maspin was accumulated over time. On day 3, as cells went into exponential growth, the concentration of secreted maspin was estimated to be 0.15 $\mu g/10^6$ cells/ml. In all the detachment experiments, the remaining adherent cells showed no sign of apoptosis as judged by poly(ADP-ribose) polymerase cleavage assay and caspase activity assays (data not shown). This

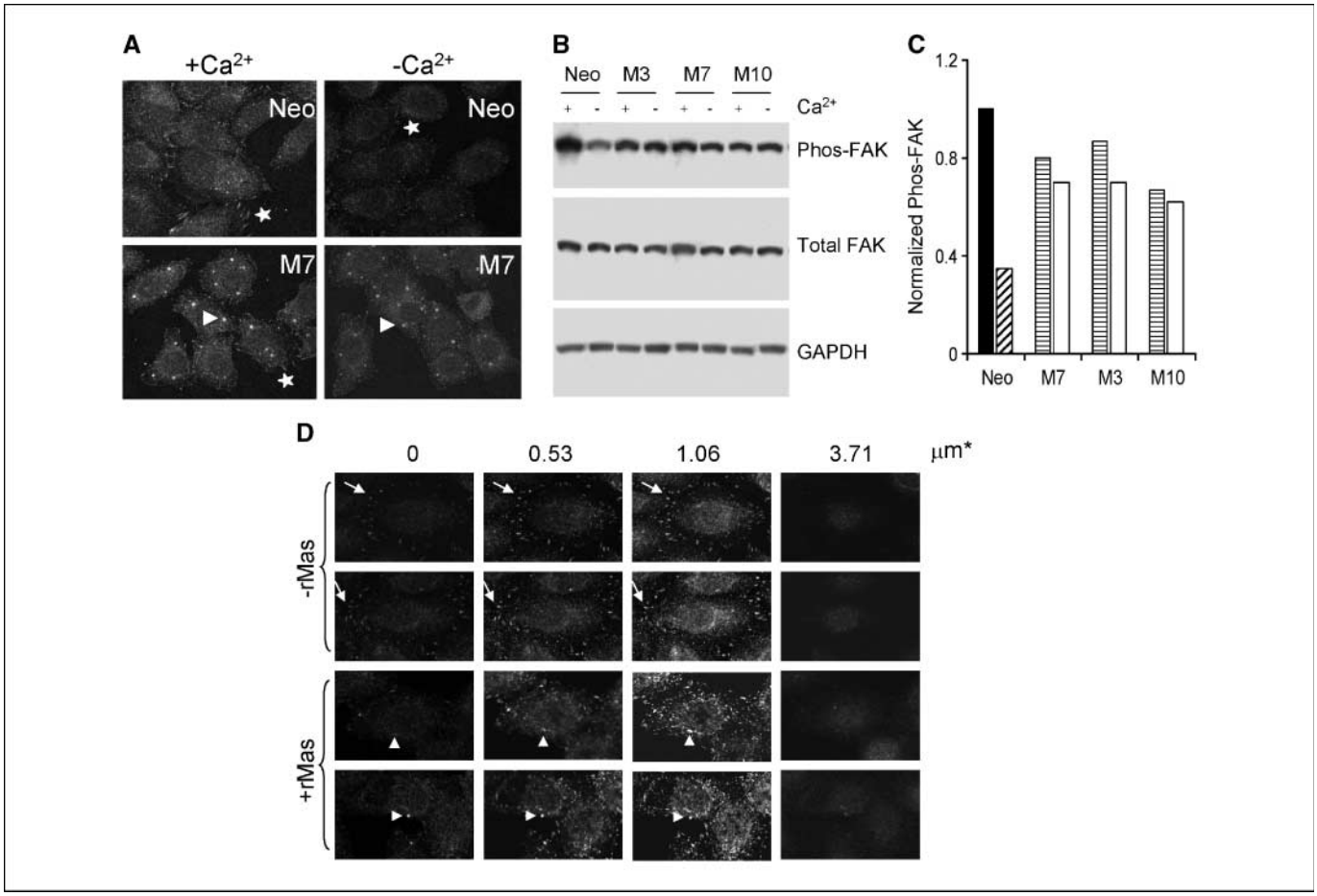

Figure 2. Maspin alters phospho-FAK distribution and stability. *A,* immunofluorescent staining of phospho-FAK in Neo cells and M7 cells before and after the detachment treatment. *Stars,* phospho-FAK associated with fibrillar cell membrane protrusion in both Neo cells and maspin-transfected M7 cells. *Arrows,* distinct dense staining of phospho-FAK in maspin-transfected M7 cells that are not associated with the fibrillar cell membrane protrusion. Magnification, ×1,000. *B,* Western blot of phospho-FAK, total-FAK, and glyceraldehyde-3-phosphate dehydrogenase (*GAPDH*) in transfected DU145 cells before and after the detachment treatment. A total of 30 μg of cell lysate was loaded into each lane. *C,* densitometric values of phospho-FAK Western blots (*B*) were normalized against the values of corresponding glyceraldehyde-3-phosphate dehydrogenase. The normalized phospho-FAK value for Neo cells before the detachment treatment (■) was then used as the baseline to calculate the relative abundance of phospho-FAK in post-detachment Neo cells (▤), in maspin-transfected clonal cell lines before the detachment (▨), and in maspin-transfected clonal cell lines after the detachment (□). *D,* confocal imaging of immunofluorescent staining of phospho-FAK in DU145 cells before and after the treatment with rMaspin (10 μg/mL in culture medium for 24 hours). Two representative fields of each cell population were selected. From each field, four planery confocal images at the indicated distances from the basal surface (*μm**). →, phospho-FAK associated with fibrillar cell membrane protrusion in untreated DU145 cells. ▷, distinct dense staining of phospho-FAK in rMaspin-treated DU145 cells that are not associated with the fibrillar cell membrane protrusion. Magnification, ×1,000.

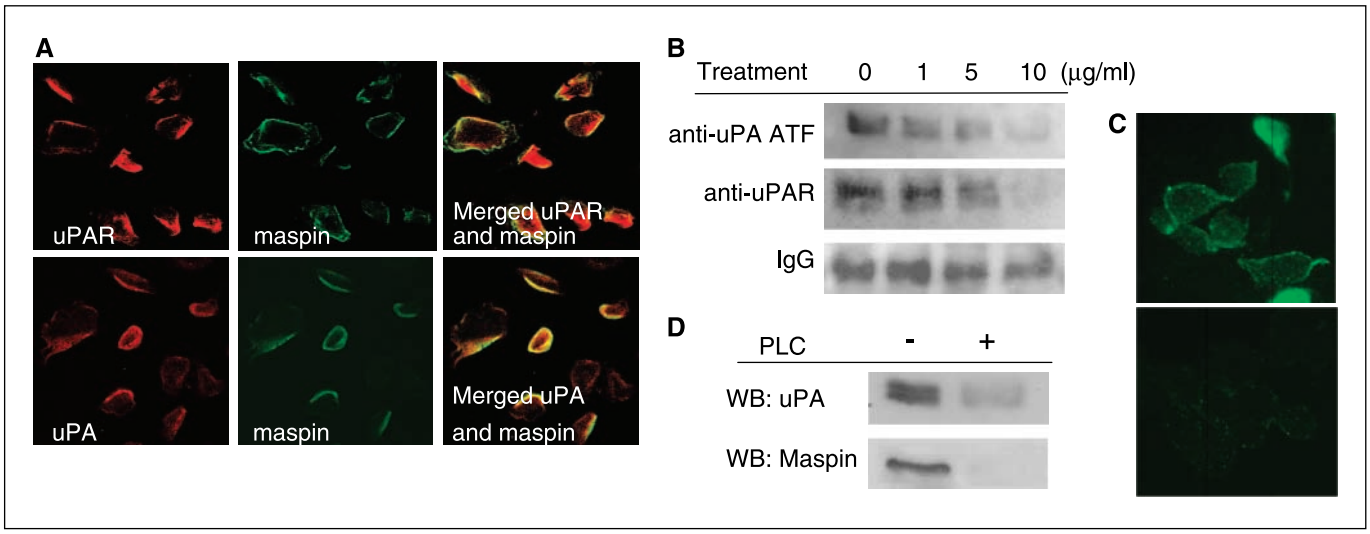

Figure 3. rMaspin binds to uPA/uPAR on DU145 cell surface. *A,* confocal images of DU145 cells treated with 20 μg/mL rMaspin at 4°C (for 1 hour) were immunofluorescently stained for uPA, uPAR, and maspin. All the immunostainings were done with unpermeablized cells. Magnification, ×620. *B,* Western blot (*WB*) of rMaspin bound to DU145 cells that had been previously treated with anti-uPA ATF, anti-uPAR, or preimmune IgG at the indicated concentrations. *C,* immunostaining of rMaspin bound to DU145 cells that had been pretreated with preimmune IgG (*top*), or anti-uPA ATF and anti-uPAR (*bottom*). Magnification, ×620. *D,* Western blot of uPA and rMaspin bound to the DU145 cells before (−) and after (+) PLC treatment.

is not surprising because more strenuous cation chelation by EDTA is a commonly used benign procedure to detach cells in culture. Thus, we believe that the cell detachment in our experiments resulted directly from the physical dissociation of preexisting cell-matrix contacts, rather than from cell death–provoked changes.

A barrier to dissociate cells from ECM is the strength of cell-ECM association, which depends, at least in part, on the temporal and spatial regulation of FACs. At the center is FAK, which undergoes autophosphorylation at Tyr^{397} (Y^{397}) residue when activated by ECM-engaged integrins (19, 20). Our immunofluorescent staining showed that phospho-FAK was organized into thin fibrilar fragments in Neo cells, especially pronounced at the cell periphery (Fig. 2*A*). In contrast, the phospho-FAK staining pattern in M7 cells had a distinct dense and punctate pattern throughout the cell body. Upon detachment treatment, the intensity of phospho-FAK in Neo cells was greatly reduced but largely unchanged in M7 cells. As shown in Fig. 2*B* and *C*, Western blot detected a higher basal level of phospho-FAK in Neo cells than in M cells. Consistent with the immunostaining results, after the detachment treatment, the level of phospho-FAK in Neo cells was significantly reduced, whereas the level of phospho-FAK in M cells remained unchanged. To further confirm the specificity of the maspin effect on the dynamics of phospho-FAK–dependent FACs, we treated DU145 cells with rMaspin. As shown by the planery confocal immunofluorescent images in Fig. 2*D*, untreated control cells featured basolateral fibrillar phospho-FAK stains aligned with cell membrane protrusion fronts. In contrast, rMaspin-treated DU145 cells exhibited dense and punctate basolateral phospho-FAK stains that were away from the cell membrane protrusions.

Effect of maspin on cell surface–associated uPA/uPAR complex. To better understand the molecular mechanism by which maspin exerts spatial and temporal regulation of FACs, it is essential to identify the molecular target of maspin. Because maspin is a cell surface–associated and a secreted protein, it may have an extracellular mode of action. To this end, uPA is the only extracellular partner of maspin thus far implicated. Immunostaining revealed colocalization of rMaspin with both uPA and uPAR on DU145 cell surface (Fig. 3*A*). Conversely, anti-uPA ATF and anti-uPAR that have been shown to disrupt the uPA/uPAR interaction dose-dependently inhibited the binding of rMaspin to DU145 cell surface, as judged by Western blot (Fig. 3*B*) and immunofluorescent staining (Fig. 3*C*). Cell surface–associated rMaspin and uPA were concomitantly reduced upon PLC treatment (Fig. 3*D*) that has been shown to remove glycosylphosphotidylinositol-anchored uPAR.

At 4°C, a low level of rMaspin internalization was detected under a mild permeabilizing condition (0.1% saponin; Fig. 4*A*). When the incubation temperature was shifted to 37°C (permitting internalization), most of the exogenously added rMaspin was internalized along with uPA and uPAR. Consistent with an earlier report (32), immunostaining detected the association of internalized uPA (and uPAR; data not shown) with lysosomal vesicles under a strong permeabilizing condition (Triton X-100; Fig. 4*A, inset*). The concomitant internalization of rMaspin, uPA, and uPAR increased over time. In a reciprocal fashion, rMaspin and uPA were continuously depleted from the cell surface (Fig. 4*B*). The subcellular distribution of uPA and uPAR was not significantly affected by the temperature shift in the absence of rMaspin. We also treated DU145 cells sequentially with uPAR antibody and rMaspin followed by reverse cell surface protein biotinylation and streptavidin pull-down. As shown in Fig. 4*C* and *D*, uPAR antibody significantly induced uPA and uPAR internalization but prevented maspin binding and internalization (Fig. 4*D*). This data further support that maspin internalization is dependent on the uPA/uPAR complex.

In complementary experiments, treatment of M7 cells with Abs4A resulted in a dose-dependent increase of cell surface–associated uPA and uPAR and increased uPA secretion (Fig. 5*A*). Treatment of M7 and M10 cells with anti-uPA ATF or anti-uPAR reduced cell surface–associated maspin (Fig. 5*B*). These results indicate that the cell surface association of endogenously expressed maspin depends on its RSL and on the uPA/uPAR complex. To detect the biophysical interaction between maspin and the

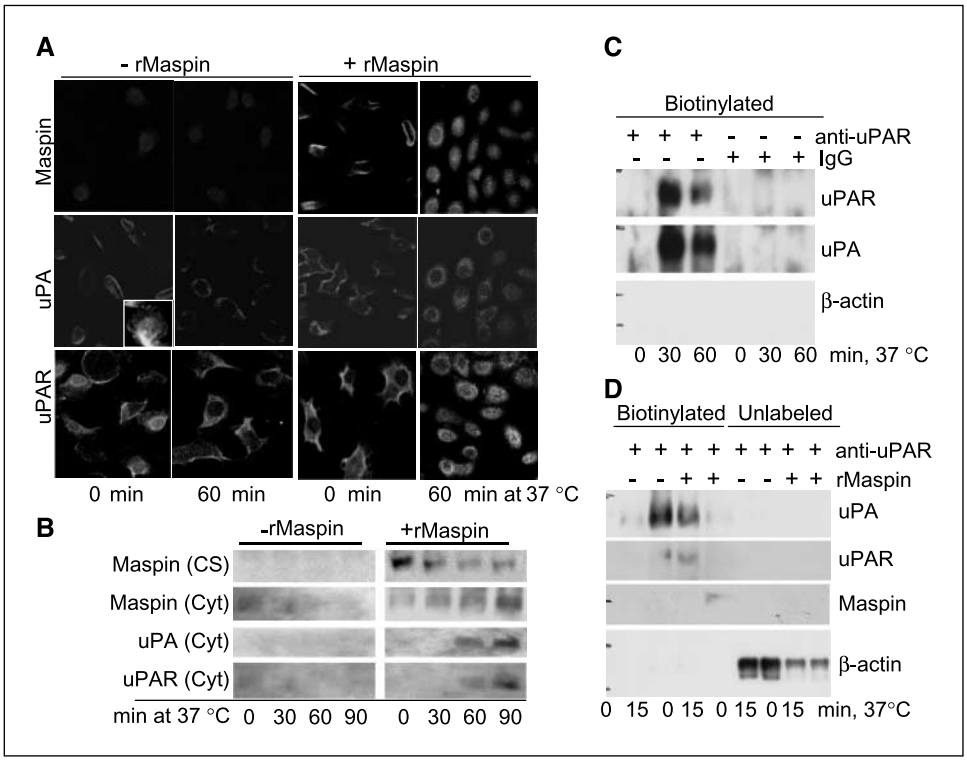

Figure 4. rMaspin readily stimulates the internalization of uPA and uPAR. *A,* representative confocal microscopic images of immunofluorescent staining of maspin, uPA, and uPAR in DU145 cells that were either untreated or treated with rMaspin (20 μg/mL) and subsequently underwent temperature shift from 4°C to 37°C for 60 minutes. The immunostainings were done with mildly permeabilized cells (0.1% saponin). *Inset,* (0 minute at 37°C) uPA staining after cells were completely permeabilized by 0.2% Triton X-100. Magnification, ×620. *B,* tracking cell surface–associated (*CS*) and cytosolic (*Cyt*) maspin, uPA, and uPAR by cell fractionation and Western blot. *C,* Western blot detection of inverse-biotinylated and internalized uPAR and uPA in DU145 cells at the indicated time points after the temperature shift to 37°C. Western blot of β-actin with the same membrane showed no contamination by unlabeled cellular proteins. *D,* Western blot detection of internalized inverse-biotinylated uPA, uPAR, and maspin in DU145 cells that were pretreated with anti-uPAR. The preexisting unlabeled cytosolic proteins analyzed alongside for uPA, uPAR, maspin, and β-actin to monitor the specificity of the reverse biotinylation.

uPA/uPAR complex, we did immunoprecipitation/Western blot. As shown in Fig. 5*C*, rMaspin added at 4°C coprecipitated with both uPA and uPAR from Neo cells. In parallel, a significant amount of endogenous maspin was coprecipitated with both uPA and uPAR from maspin-transfected cell lines. Furthermore, an increased association between LRP and uPAR correlated with either rMaspin treatment (of the Neo cells) or endogenous maspin expression (Fig. 5*C*).

Novel preference for pro-uPA. Based on the cell surface dependence of the maspin effect on uPA-mediated plasminogen activation, maspin may physically interact with pro-uPA or active-uPA. We did ELISA and equilibrium binding assays to test these possibilities. In both assays, no interaction between maspin and active uPA was detected (data not shown). However, rMaspin exhibited a significant binding to pro-uPA (Fig. 6*A, a*) but not to plasmin (Fig. 6*A, b*) in ELISA. Consistently, pro-uPA dose-dependently quenched the fluorescence of maspin^{-FL} in the equilibrium binding study (Fig. 6*B*). The profile of the binding isotherm was consistent with that of a high-affinity, noncovalent interaction with an apparent K_d of 269 ± 22 nmol/L (r^2 = 0.962). The noncovalent nature of this interaction was further confirmed by the capacity of unlabeled rMaspin to displace maspin^{-FL} from the preformed maspin^{-FL}/pro-uPA complex (Fig. 6*B, inset*).

The proteolytic activation of pro-uPA is thought to be mediated by plasmin. As shown in Fig. 6*C*, pro-uPA underwent a specific cleavage in the presence of plasmin, producing both the α-chain and β-chain of uPA. However, when pro-uPA and plasmin were incubated in the presence of rMaspin, the cleavage of pro-uPA was significantly inhibited. We generated purified Mas^{R340A} (Fig. 6*A, c*) to examine the role of maspin RSL. When tested by ELISA, Mas^{R340A} showed no affinity for pro-uPA (Fig. 6*A, a*), active uPA (data not shown), and plasmin (Fig. 6*A, b*). Mas^{R340A} had no effect on pro-uPA cleavage (Fig. 6*C*). Neither rMaspin nor Mas^{R340A} was significantly degraded by plasmin or uPA. These data suggest a critical role of maspin RSL in the interaction with pro-uPA and raised the possibility that maspin may inhibit the proteolytic activation of pro-uPA *in vivo*. To this end, maspin RSL seemed critical for protecting cells from Ca^{2+} reduction–induced detachment, because Mas^{R340A} had no effect (Fig. 6*D*). Interestingly, PAI-1, the bona fide uPA inhibitor and the potent stimulus for uPA/uPAR internalization, has been shown to slightly stimulate cell detachment (Fig. 6*D*). This PAI-1 effect may involve uPA-independent mechanisms (33). It is also worth noting that PAI-1 binds predominantly to active uPA (34).

Discussion

Cell migration involves concerted new attachment of the leading edge to ECM and detachment from the preexisting cell-matrix contacts at the trailing edge. Both cell adhesion and detachment may be associated with, and further propelled by, ECM remodeling (31). Our data in this study showed that maspin inhibited cell detachment from the preexisting contacts with their natural ECM. Furthermore, our biophysical and biochemical evidence suggests that maspin may internalize pro-uPA that is complexed with uPAR.

Motile cells are often associated with increased number of newly assembled FACs at the leading edge, whereas nonmoving cells tend to be associated with strong dotty FACs that are spread across the basolateral surface. The latter type of FACs is thought to have undergone the "maturation" process and be responsible for stabilizing cell-matrix adhesion (6, 19, 20). Our data suggest that maspin may promote FAK-dependent FAC maturation. In maspin-nonexpressing DU145 cells, the phospho-FAK immunostains were mostly radiating fibrillar fragments at the cell periphery, whereas in maspin-transfected cells or rMaspin-treated cells, the phospho-FAK stains were densely dotty and evenly spread over the basolateral surface of the cells. Upon detachment treatment, the fibrillar leading edge–associated phospho-FAK stain in mock-transfected

cells decreased significantly, which semiquantitatively correlated with a significant decrease of the phospho-FAK level as judged by Western blot. In contrast, the densely dotty phospho-FAK stains in maspin-transfected cells largely sustained the detachment treatment. Consistently, the level of phospho-FAK in maspin-transfected cells was not significantly altered by detachment.

How does maspin promote FAC maturation at the molecular level? The dynamics of FAC is regulated both by integrin-mediated outside-in signaling pathway and by small GTP-binding protein (Rho, Rac, and Cdc42)–mediated inside-out signaling pathway (35). Because rMaspin was sufficient to inhibit cell detachment, motility, and invasion, the maspin-responsive pathway must be preexisting. The identification of several housekeeping molecules as intracellular maspin partners (17, 18) raised the possibility that maspin, once internalized, may regulate the signaling pathways that control the FAC dynamics. On the other hand, it is logical to assume that the maspin internalization begins with some kind of molecular interactions on the cell surface. To this end, the uPA/uPAR complex is the only cell surface–associated target of maspin implicated thus far. Although we can not rule out the possibility that maspin may interact with other cell surface–associated molecules at this time, our evidence that disruption of uPA and uPAR interaction prevents maspin binding to the cell surface as well as maspin internalization further suggests that the cell surface–associated uPA/uPAR complex may be the primary extracellular target of maspin.

Despite the evidence that uPAR may directly bind to and regulate integrin-dependent FAC (36, 37), others have observed that LRP-mediated endocytosis of uPA and uPAR led to a substantial increase in cell surface β_1 integrin (38). Thus, it remains to be clarified whether the role of uPA/uPAR in cell-matrix interaction has to depend on direct interaction with FAC. Our evidence suggests that the regulation of uPA/uPAR by maspin may not be directly involved in FAC maturation because maspin did not have the same immunostaining pattern as phospho-FAK. Furthermore, the molecular interaction between maspin and the uPA/uPAR complex did not sustain the presence of uPAR on the cell surface. In contrast, maspin robustly stimulated the concomitant internalization of uPA and uPAR.

Both the formation and maturation of FAC may be propelled by spatially and temporally coordinated ECM remodeling. Targeting cell surface–associated uPA/uPAR complex has been shown to be particularly effective to block tumor-mediated ECM remodeling, at least in part, because plasmin derived from plasmiongen activation can directly degrade non-fibrillar ECM proteins and activate other types of proteases, such as metalloproteinases (39). It is worth noting that PAI-2, a tumor suppressive homologue of maspin that also triggers the internalization of cell surface–associated uPA/uPAR complex (40), has been shown to counteract the uPA-mediated cell detachment *in vitro* (41). Consistent with our earlier evidence that maspin inhibits tumor cell surface uPA activity (7), maspin dramatically inhibited tumor-mediated ECM degradation *in vitro* and inhibited tumor-induced bone matrix degradation in the SCID-Hu model for prostate tumor bone metastasis (6).

On the cell surface, uPAR recruits pro-uPA that is subsequently proteolytically activated, presumably, by an adjacent plasmin. Therefore, at a steady state, whereas some cell surface–anchored uPAR may be occupied by active uPA, other uPARs may be either unoccupied or occupied by pro-uPA. A long-standing question has been how maspin inhibits the uPA/uPAR complex if it does not act as a proteolytic inhibitor. To this end, our ELISA and equilibrium binding assays showed that rMaspin specifically bound to pro-uPA but not active uPA or plasmin via a noncovalent interaction. This is the first evidence that a serpin prefers the zymogen form of uPA. Interestingly, pro-uPA has a low intrinsic reactivity to activate plasminogen. This activity is thought to be responsible for sustaining a reciprocal uPA-plasminogen activation loop (34). Currently, it is not known how the intrinsic activity of pro-uPA is

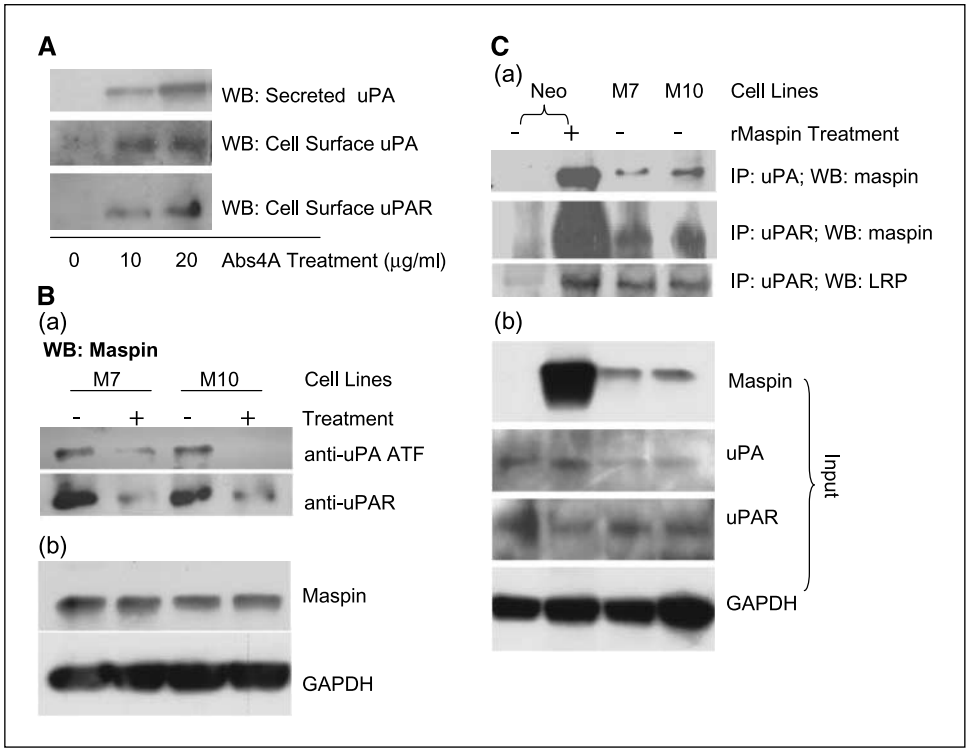

Figure 5. Binding of maspin to the uPA/uPAR complex depends on its RSL and enhances the interaction with LRP. *A,* Western blot (*WB*) of biotinylated cell surface–associated uPA and uPAR and secreted uPA in M7 cells that were treated with Abs4A at the indicated concentrations. *B,* cell surface–association of maspin depends on uPA and uPAR. *a,* Western blot of cell surface–associated maspin in M7 and M10 cells that were treated with or without anti-uPA ATF and anti-uPAR, respectively. *b,* Western blot of the total level of maspin along with the internal control of glyceraldehyde-3-phosphate dehydrogenase (*GAPDH*) in cells treated with anti-uPA ATF or anti-uPAR. *C,* immunoprecipitation (*IP*)/Western blot detection of protein-protein associations. *a,* Western blot of rMaspin, endogenous maspin, or LRP in the immune complex with uPA or uPAR. *b,* Western blot of maspin, uPA, uPAR, and glyceraldehyde-3-phosphate dehydrogenase input in the total lysates of untreated Neo cells, rMaspin-treated Neo cells, M7 cells, and M10 cells.

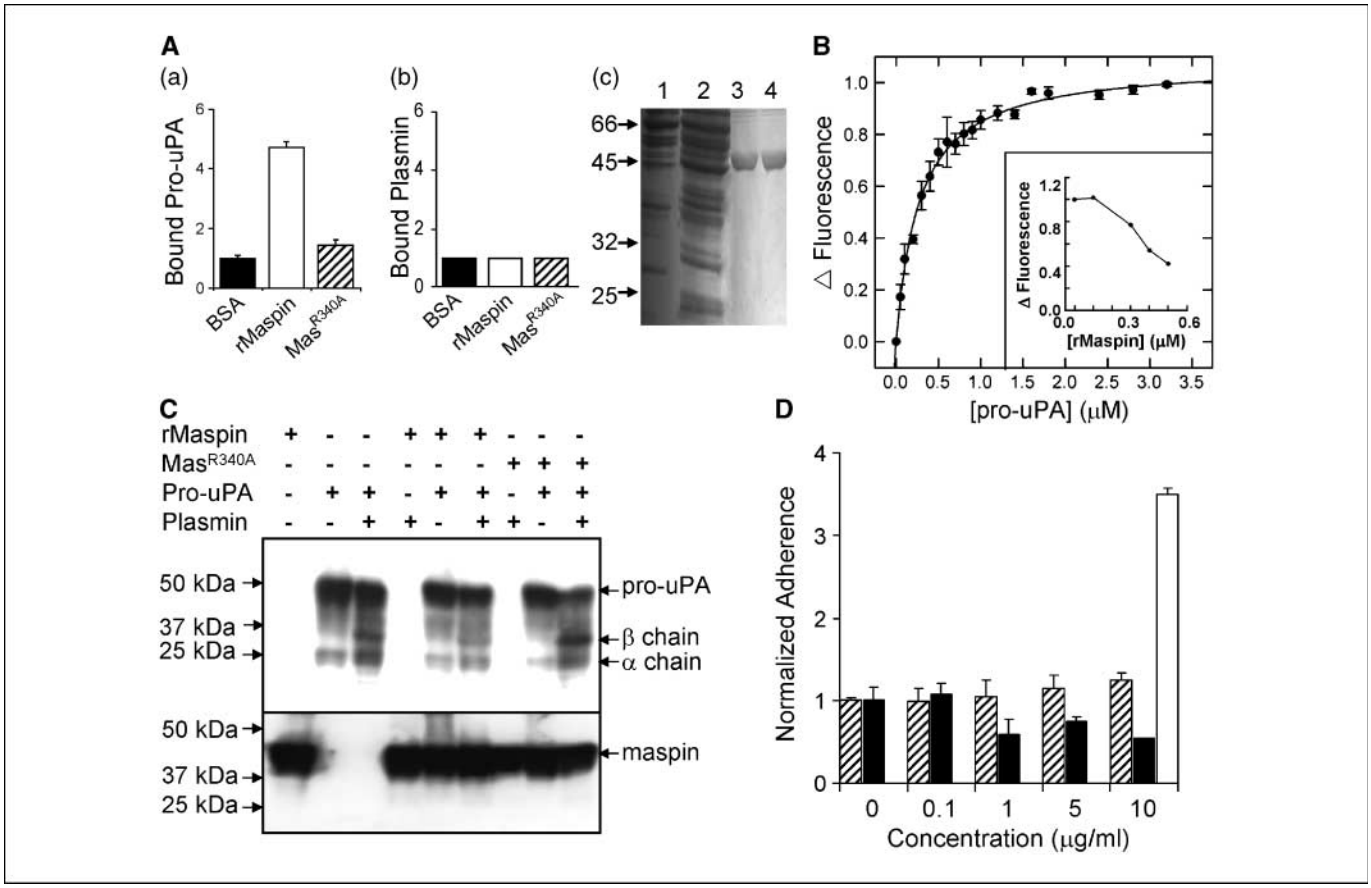

Figure 6. A critical role of maspin RSL in the interaction with pro-uPA, the inhibition of pro-uPA cleavage, and the inhibition of cell detachment. *A,* ELISA detection of protein-protein interaction. *a,* ELISA detection of rMaspin and Mas^{R340A} bound to immobilized pro-uPA. The bindings of rMaspin and Mas^{R340A} were normalized against that of BSA and are presented as fold differences. *b,* ELISA detection of rMaspin and Mas^{R340A} bound to immobilized plasmin. The bindings of rMaspin and Mas^{R340A} were normalized against that of BSA and are presented as fold differences. *c,* Coomassie blue–stained SDS-PAGE loaded with 50 μg lysate of insect cells infected with the mock baculovirus (*lane 1*), 50 μg lysate of insect cells infected with Mas^{R340A}-encoding baculovirus (*lane 2*), 5 μg purified Mas^{R340A} (*lane 3*), and 5 μg purified rMaspin (*lane 4*). Molecular weight standards (*left*). *B,* equilibrium binding of pro-uPA to maspin^{-FL}. Changes of fluorescence of maspin^{-FL} are plotted against the concentration of pro-uPA. *Inset,* dose-dependent replacement of pro-uPA-bound maspin^{-FL} (formed by incubating 10 nmol/L maspin^{-FL} and 50 nmol/L pro-uPA) by unlabeled rMaspin. *C,* effects of rMaspin and Mas^{R340A} on *in vitro* plasmin-mediated pro-uPA cleavage. Proteins resulting from the indicated reaction conditions were resolved by nonreducing SDS-PAGE for Western blot analyses. The same membrane was probed for both uPA (*top*) and maspin (*bottom*). *D,* effects of Mas^{R340A} and rPAI-1 on DU145 detachment. Adherent DU145 cells were analyzed by the sulforhodamine B assay after the detachment treatment in the presence of Mas^{R340A} (▨) and rPAI-1 (■) at the indicated concentrations. The cell adherence data were normalized against the control data obtained with BSA at the corresponding concentrations. The result of a parallel detachment experiment in the presence of 20 μg/mL rMaspin (□) is included as a reference. *Columns/points,* averages of four independent titrations; *bars,* SE. SEs are not shown in the inset of (*C*) for clarity.

enzymatically controlled. In our hands, rMaspin inhibited plasmin-mediated proteolytic cleavage of pro-uPA. Furthermore, Mas^{R340A} that failed to bind to pro-uPA did not inhibit plasmin-mediated pro-uPA cleavage and did not inhibit cell detachment. The effects of maspin are not likely to be limited to the step of pro-uPA activation. We showed that maspin increased the interaction between uPAR and LRP and the internalization of uPA and uPAR. Others have shown that pro-uPA and active uPA can be both internalized by the LRP-mediated mechanism (42). It is intriguing to speculate that maspin may quench cell surface–associated uPA/uPAR complex via the LRP-mediated internalization even before pro-uPA is converted to active two-chain uPA.

Our kinetic analyses revealed a nanomolar K_d value for the interaction of maspin^{-FL} with soluble pro-uPA. The robust maspin-mediated internalization prohibits similar "equilibrium" analyses for binding kinetics on the cell surface. We speculate that the biological effect of endogenous maspin on cell surface–associated uPA/uPAR may be sustained by active protein synthesis and secretion, whereas much higher concentrations of purified maspin may be needed to achieve similar effects on maspin-nonexpressing cells due to the one-way straight internalization. In deed, we found that the effective rMaspin concentration for inhibiting the detachment, motility, and invasion of DU145 cells was 5 to 10 times higher than the accumulated endogenously secreted maspin in normal prostate epithelial cell culture. The need for excessive supply of purified maspin may be a pharmacologic concern when considering maspin as a potential therapeutic agent. However, an earlier study using a slow-release capsule to increase maspin local concentration achieved specific inhibition of prostate tumor growth and tumor-induced angiogenesis *in vivo* (14).

Acknowledgments

Received 9/30/2005; revised 12/28/2005; accepted 2/14/2006.

Grant support: NIH grants CA84176 (S. Sheng) and F31CA110211 (J. Lockett), Ruth Sager Memorial Fund (S. Sheng), Fund for Cancer Research (S. Sheng), and Department of Defense grant DAMD17-03-1-0038 (S. Yin).

The costs of publication of this article were defrayed in part by the payment of page charges. This article must therefore be hereby marked *advertisement* in accordance with 18 U.S.C. Section 1734 solely to indicate this fact.

References

1. Bartuski AJ, Kamachi Y, Schick C, Overhauser J, Silverman GA. Cytoplasmic antiproteinase 2 (PI8) and bomapin (PI10) map to the serpin cluster at 18q21.3. Genomics 1997;43:321–8.
2. Schneider SS, Schick C, Fish KE, et al. A serine proteinase inhibitor locus at 18q21.3 contains a tandem duplication of the human squamous cell carcinoma antigen gene. Proc Natl Acad Sci U S A 1995;92:3147–51.
3. Zou Z, Anisowicz A, Hendrix MJ, et al. Maspin, a serpin with tumor-suppressing activity in human mammary epithelial cells. Science 1994;263:526–9.
4. Sheng S. The promise and challenge toward the clinical application of maspin in cancer. Front Biosci 2004;9:2733–45.
5. Seftor RE, Seftor EA, Sheng S, Pemberton PA, Sager R, Hendrix MJ. maspin suppresses the invasive phenotype of human breast carcinoma. Cancer Res 1998;58:5681–5.
6. Cher ML, Biliran HR, Jr., Bhagat S, et al. Maspin expression inhibits osteolysis, tumor growth, and angiogenesis in a model of prostate cancer bone metastasis. Proc Natl Acad Sci U S A 2003;100:7847–52.
7. Biliran H, Jr., Sheng S. Pleiotrophic inhibition of pericellular urokinase-type plasminogen activator system by endogenous tumor suppressive maspin. Cancer Res 2001;61:8676–82.
8. Odero-Marah VA, Khalkhali-Ellis Z, Chunthapong J, et al. Maspin regulates different signaling pathways for motility and adhesion in aggressive breast cancer cells. Cancer Biol Ther 2003;2:398–403.
9. Sager R, Sheng S, Anisowicz A, et al. RNA genetics of breast cancer: maspin as paradigm. Cold Spring Harb Symp Quant Biol 1994;59:537–46.
10. Sheng S, Carey J, Seftor EA, Dias L, Hendrix MJ, Sager R. Maspin acts at the cell membrane to inhibit invasion and motility of mammary and prostatic cancer cells. Proc Natl Acad Sci U S A 1996;93:11669–74.
11. Sheng S, Pemberton PA, Sager R. Production, purification, and characterization of recombinant maspin proteins. J Biol Chem 1994;269:30988–93.
12. Shi HY, Zhang W, Liang R, et al. Modeling human breast cancer metastasis in mice: maspin as a paradigm. Histol Histopathol 2003;18:201–6.
13. Zhang M, Shi Y, Magit D, Furth PA, Sager R. Reduced mammary tumor progression in WAP-TAg/WAP-maspin bitransgenic mice. Oncogene 2000;19:6053–8.
14. Zhang M, Volpert O, Shi YH, Bouck N. Maspin is an angiogenesis inhibitor. Nat Med 2000;6:196–9.
15. Liu J, Yin S, Reddy N, Spencer C, Sheng S. Bax mediates the apoptosis-sensitizing effect of maspin. Cancer Res 2004;64:1703–11.
16. Jiang N, Meng Y, Zhang S, Mensah-Osman E, Sheng S. Maspin sensitizes breast carcinoma cells to induced apoptosis. Oncogene 2002;21:4089–98.
17. Yin S, Li X, Meng Y, et al. Tumor suppressive maspin regulates cell response to oxidative stress by direct interaction with glutathione *S*-transferase. J Biol Chem 2005;280:34985–96.
18. Bailey CM, Khalkhali-Ellis Z, Kondo S, et al. Maspin binds directly to interferon regulatory factor 6: identification of a novel serpin partnership. J Biol Chem 2005; 280:34210–7.
19. Zamir E, Geiger B. Molecular complexity and dynamics of cell-matrix adhesions. J Cell Sci 2001;114: 3583–90.
20. Schlaepfer DD, Mitra SK. Multiple connections link FAK to cell motility and invasion. Curr Opin Genet Dev 2004;14:92–101.
21. McGowen R, Biliran H, Jr., Sager R, Sheng S. The surface of prostate carcinoma DU145 cells mediates the inhibition of urokinase-type plasminogen activator by maspin. Cancer Res 2000;60:4771–8.
22. Sheng S. The urokinase-type plasminogen activator system in prostate cancer metastasis. Cancer Metastasis Rev 2001;20:287–96.
23. Sidenius N, Blasi F. The urokinase plasminogen activator system in cancer: recent advances and implication for prognosis and therapy. Cancer Metastasis Rev 2003;22:205–22.
24. Keepers YP, Pizao PE, Peters GJ, van Ark-Otte J, Winograd B, Pinedo HM. Comparison of the sulforhodamine B protein and tetrazolium (MTT) assays for *in vitro* chemosensitivity testing. Eur J Cancer 1991;27: 897–900.
25. Salonen EM, Vaheri A, Pollanen J, et al. Interaction of plasminogen activator inhibitor (PAI-1) with vitronectin. J Biol Chem 1989;264:6339–43.
26. Webber MM, Bello D, Kleinman HK, Hoffman MP. Acinar differentiation by non-malignant immortalized human prostatic epithelial cells and its loss by malignant cells. Carcinogenesis 1997;18:1225–31.
27. Olson ST, Bock PE, Kvassman J, et al. Role of the catalytic serine in the interactions of serine proteinases with protein inhibitors of the serpin family. Contribution of a covalent interaction to the binding energy of serpin-proteinase complexes. J Biol Chem 1995;270: 30007–17.
28. Yin X, Zhang H, Burrows F, Zhang L, Shores CG. Potent activity of a novel dimeric heat shock protein 90 inhibitor against head and neck squamous cell carcinoma *in vitro* and *in vivo*. Clin Cancer Res 2005;11:3889–96.
29. Bradford DS, Foster RR, Nossel HL. Coagulation alterations, hypoxemia, and fat embolism in fracture patients. J Trauma 1970;10:307–21.
30. Abraham S, Zhang W, Greenberg N, Zhang M. Maspin functions as tumor suppressor by increasing cell adhesion to extracellular matrix in prostate tumor cells. J Urol 2003;169:1157–61.
31. Friedl P, Wolf K. Tumour-cell invasion and migration: diversity and escape mechanisms. Nat Rev Cancer 2003;3:362–74.
32. Bastholm L, Elling F, Brunner N, Nielsen MH. Immunoelectron microscopy of the receptor for urokinase plasminogen activator and cathepsin D in the human breast cancer cell line MDA-MB-231. APMIS 1994;102:279–86.
33. Czekay RP, Aertgeerts K, Curriden SA, Loskutoff DJ. Plasminogen activator inhibitor-1 detaches cells from extracellular matrices by inactivating integrins. J Cell Biol 2003;160:781–91.
34. Behrendt N, List K, Andreasen PA, Dano K. The prourokinase plasminogen-activation system in the presence of serpin-type inhibitors and the urokinase receptor: rescue of activity through reciprocal proenzyme activation. Biochem J 2003;371:277–87.
35. Hood JD, Cheresh DA. Role of integrins in cell invasion and migration. Nat Rev Cancer 2002;2:91–100.
36. Chapman HA, Wei Y. Protease crosstalk with integrins: the urokinase receptor paradigm. Thromb Haemost 2001;86:124–9.
37. Blasi F, Carmeliet P. uPAR: a versatile signalling orchestrator. Nat Rev Mol Cell Biol 2004;3:932–43.
38. Salicioni AM, Gaultier A, Brownlee C, Cheezum MK, Gonias SL. Low density lipoprotein receptor-related protein-1 promotes β_1 integrin maturation and transport to the cell surface. J Biol Chem 2004;279:10005–12.
39. Mueller BM. Different roles for plasminogen activators and metalloproteinases in melanoma metastasis. Curr Top Microbiol Immunol 1996;213:65–80.
40. Tsatas D, Baker MS, Rice GE. Tissue-specific expression of the relaxed conformation of plasminogen activator inhibitor-2 and low-density lipoprotein receptor-related protein in human term gestational tissues. J Histochem Cytochem 1997;45:1593–602.
41. Reinartz J, Schaefer B, Bechtel MJ, Kramer MD. Plasminogen activator inhibitor type-2 (PAI-2) in human keratinocytes regulates pericellular urokinase-type plasminogen activator. Exp Cell Res 1996;223:91–101.
42. Kounnas MZ, Henkin J, Argraves WS, Strickland DK. Low density lipoprotein receptor-related protein/alpha 2-macroglobulin receptor mediates cellular uptake of pro-urokinase. J Biol Chem 1993;268:21862–7.